Quantum chemical studies of dioxygen activation by mononuclear non-heme iron enzymes with the 2-His-1-carboxylate facial triad

ARTICLE *in* DALTON TRANSACTIONS · NOVEMBER 2004

Impact Factor: 4.2 · DOI: 10.1039/B408340G · Source: PubMed

3 AUTHORS, INCLUDING:

Tomasz Borowski
Instytut Katalizy i Fizykochemii Powierzchni i…
45 PUBLICATIONS **1,206** CITATIONS

SEE PROFILE

PERSPECTIVE

Dalton
www.rsc.org/dalton

Quantum chemical studies of dioxygen activation by mononuclear non-heme iron enzymes with the 2-His-1-carboxylate facial triad

Arianna Bassan, Tomasz Borowski and Per E. M. Siegbahn*
Department of Physics, Stockholm University, SE 106 91 Stockholm, Sweden

Received 2nd June 2004, Accepted 5th August 2004
First published as an Advance Article on the web 27th August 2004

Density functional theory with the B3LYP hybrid functional has been used to study the mechanisms for dioxygen activation by four families of mononuclear non-heme iron enzymes: α-ketoacid-dependent dioxygenases, tetrahydrobiopterin-dependent hydroxylases, extradiol dioxygenases, and Rieske dioxygenases. These enzymes have a common active site with a ferrous ion coordinated to two histidines and one carboxylate group (aspartate or glutamate). In contrast to the heme case, this type of weak field environment always leads to a high-spin ground state. With the exception of the Rieske dioxygenases, which have an electron source outside the active site, the dioxygen activation process passes through the formation of a bridging-peroxide species, which then undergoes O–O bond cleavage finally leading to the four electron reduction of O_2. In the case of tetrahydrobiopterin- and α-ketoacid-dependent enzymes, the O–O heterolysis yields a high-valent iron–oxo species, which is capable of performing a two-electron oxidation chemistry on various organic substrates. For the other two families of enzymes (extradiol dioxygenases and Rieske dioxygenases) the substrate oxidation and the O–O bond cleavage are found to be coupled. In the extradiol dioxygenases the product of the O–O bond cleavage is a ferric iron with an oxy-substrate with a mixture of radical and anionic character, which is essential for the selectivity of the catechol cleavage.

1 Introduction

Metalloproteins containing iron are involved in a wide variety of biological processes.[1,2] The versatility of iron is one main reason behind the important role played by this metal in many living organisms. The chemical properties of iron and in particular its redox potential can be finely tuned by an appropriate coordination environment. Iron in metalloproteins is usually present as Fe^{II} and Fe^{III}, which in turn can exist in high- and low-spin configurations depending on the ligand field.[1–4] The high-spin is usually the ground state when iron is coordinated by oxygen and nitrogen ligands such as the side chains of histidine, tyrosine, aspartate and glutamate.[3,5,6] It is customary to classify iron containing enzymes with this type of coordination under the name of non-heme iron proteins in contrast to the other two main groups, the heme iron proteins and the iron–sulfur proteins.[7]

The majority of the non-heme iron proteins exploits the oxidative power of dioxygen, whose uncatalyzed reactions with organic molecules are thermodynamically favorable but kinetically slow. The reason is that dioxygen has a triplet ground state and therefore any reaction between $^3O_2$ and singlet organic substrates is spin-forbidden. Nature employs mono- and binuclear non-heme iron proteins to catalyze a broad spectrum of different oxidative reactions such as desaturations, oxidative cyclizations, mono-oxygenations and dioxygenations, hydroperoxidations and epoxidations.[3] Among mononuclear non-heme iron enzymes, there exist several apparently unrelated proteins, where iron is coordinated by a common structural motif, the so-called 2-His-1-carboxylate facial triad.[8–10] More specifically iron(II) is anchored in the active site by imidazole groups of the histidines and the carboxylate group of an aspartate or glutamate, while some water ligands may complete the metal coordination. Four families of enzymes containing this structural coordination pattern have been identified: α-ketoacid-

Arianna Bassan received her undergraduate degree in chemistry at University of Padova (Italy). In 2004, she received her PhD degree at Stockholm University with a thesis entitled 'Theoretical studies of mononuclear non-heme active sites'. She is currently a postdoctoral associate in the laboratory of Prof. Per E. M. Siegbahn.

Tomasz Borowski received his MSc (1998) and PhD (2003) at Jagiellonian University, Krakow, Poland, under the supervision of Prof. Ewa Broclawik. In March 2003 he undertook post-doctoral work with Per E. M. Siegbahn at Stockholm University. His research interest focuses on the elucidation of bioinorganic reaction mechanisms, especially the catalytic mechanisms of metalloenzymes.

Per E. M. Siegbahn received his PhD degree at Stockholm University in 1973 and is currently on its staff as Full Professor in quantum chemistry. His interests have varied over the years from the development of ab initio quantum chemical methods, to the application of gas-phase reactions of small molecules, to models of heterogeneous catalysis, to his present main interest in mechanisms for redox active enzymes.

Arianna Bassan

Tomasz Borowski

Per E. M. Siegbahn

DOI: 10.1039/b408340g

dependent enzymes, pterin-dependent hydroxylases, extradiol dioxygenases and Rieske dioxygenases. The corresponding catalytic activities of these enzymes, which use dioxygen to perform various oxidative reactions, are summarized in Fig. 1, where possible reaction pathways for the chemical transformations of interest are also described. The α-ketoacid-dependent enzymes are involved in many crucial metabolic transformations and they usually employ 2-oxoglutarate (α-ketoglutarate) as co-substrate, which binds at the metal complex and which supplies two of the four electron required to fully reduce O_2.[11–13] Similarly, tetrahydrobiopterin-dependent hydroxylases use a cofactor, namely, pterin, whose hydroxylation is coupled to the hydroxylation of the main substrate, an aromatic amino acid.[14–16] Extradiol-cleaving catechol dioxygenases are isolated from soil bacteria and they catalyze the degradation of aromatic rings through the oxidative cleavage of the catecholic compounds.[17,18] Rieske dioxygenases, the fourth family shown in Fig. 1, are also found in soil bacteria and they start the catabolism of aromatic compounds yielding the corresponding *cis*-dihydrodiols,[19,20] as for example *cis*-(1*R*,2*S*)-dihydroxy-1,2-dihydronaphthalene in the case of naphthalene 1,2-dioxygenase.[21,22]

It is useful to observe that possible intermediates in dioxygen activation by iron(II) complexes are, for example: iron(II/III)–superoxo, iron(II/III/IV)–peroxo, and iron(IV/V)–oxo species. The iron(II)–superoxo species is formed when dioxygen binds to iron and an electron is provided by an external source; the iron(III)–superoxo species instead requires that iron itself carries out the one-electron reduction of dioxygen. An iron(IV)–peroxo species originates from a two-electron reduction of O_2 provided that all the reducing equivalents are supplied by iron. However, if the metal donates only one electron, an iron(III)–peroxo species can be obtained when another electron donor completes the two-electron reduction of dioxygen. Finally, an iron(II)-peroxide may be formed if both electrons are supplied from the outside.

In analogy to the generally accepted mechanism for heme oxygenases, where a high-valent iron–oxo species is involved,[4] non-heme iron oxygenases may also employ the Fe^{II} /Fe^{IV} redox couple. In the specific case of Rieske dioxygenases an even higher oxidation state has been proposed for iron, namely, Fe^{V}, associated with the Fe^{III} /Fe^{V} redox couple.[10,23] It has long been debated whether high-valent iron–oxo species could be obtained for a non-heme environment. Recently, experimental evidence has been accumulating in support for the existence of non-heme high-valent iron–oxo complexes. Particularly, Fe^{IV}=O complexes has been characterized and also isolated in the case of model complexes with ligands mimicking the non-heme environment of the enzymes.[24,25] Moreover, experimental studies on taurine/α-ketoglutarate dioxygenase have shown that the enzymatic mechanism involves a high-spin iron(IV) species capable of hydrogen atom abstraction;[26,27] strong evidence that this species corresponds to an Fe^{IV}=O intermediate comes from resonance Raman spectroscopy.[28]

The present work reviews theoretical studies undertaken in our group to shed light on the dioxygen activation process and the related oxidative reactions occurring in the four families of enzymes shown in Fig. 1. In our investigations density functional theory (DFT) has been used to elucidate the strategy adopted by the mononuclear non-heme iron enzymes to carry out the four-electron reduction of O_2. Intermediates and transition states have been located to identify which ones of the species mentioned above are likely to be involved in catalysis.

2 Computational methods

The reaction pathways of interest were investigated by means of hybrid DFT and more specifically with the B3LYP exchange correlation functional.[29–31] The two quantum chemical programs Gaussian[32] and Jaguar[33] were used. The quantum mechanical models were constructed employing the available experimental structures of the active sites of the enzymes under investigation. Relevant amino acids were usually included in the form of suitable smaller molecules, and, for example, histidine was modeled as imidazole or 4-methylimidazole, and aspartate (or the glutamate) as acetate or formate. The rigidity of the active site was sometimes reproduced by freezing some atoms according to the available X-ray data. This procedure is useful especially when the system contains molecules that are not anchored in the first coordination sphere of the metal. Having set up a model, the exploration of the appropriate potential energy surfaces (*i.e.*, the dependence of the energy on the nuclear coordinates) made it possible to examine different reaction mechanisms, which have been accepted or dismissed on the basis of the computed energies.

Molecular Hessians of reactants, intermediates and transition states were usually calculated in order to derive the zero point effects and the thermal corrections to the total energy, enthalpy and Gibbs free energy. The calculation of molecular Hessians for the transition state structures was also needed to confirm that the structure is characterized by only one imaginary frequency corresponding to the normal mode associated

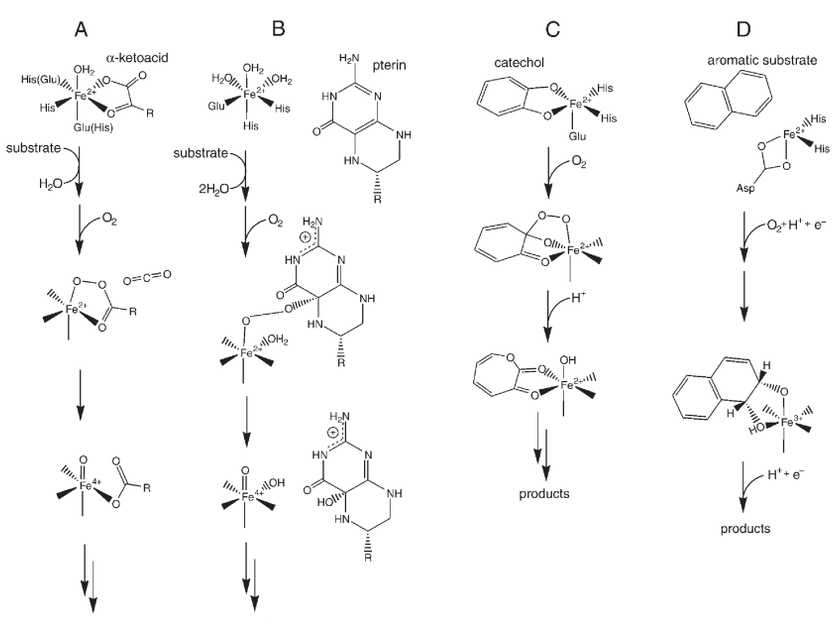

Fig. 1 Experimentally proposed mechanisms for the enzymatic reactions of **A** α-ketoacid-dependent enzymes, **B** tetrahydrobiopterin-dependent hydroxylases, **C** extradiol dioxygenases, and **D** Rieske dioxygenases.

with the reaction coordinate. When some atoms in the model are constrained according to the available X-ray data, evaluation of the thermal effects is not sufficiently accurate. In these cases, only the energy changes corrected for the zero-point effects were derived and with good approximation they reflect the enthalpy profile. Standard double zeta basis sets were employed for geometry optimizations and for the evaluations of zero point effects and thermal corrections. However, the final energies for the fully optimized structures were calculated with larger basis sets including polarization functions on all atoms. Solvent effects were derived by modeling the solvent as a macroscopic continuum[34,35] with dielectric constant $\varepsilon = 4$ and they were usually evaluated at the same level of theory as the geometry optimizations.

3 Dioxygen binding and activation

On the basis of theoretical investigations, the catalytic mechanisms proposed for the four families of non-heme iron enzymes (α-ketoacid-dependent dioxygenases, pterin-dependent hydroxylases, extradiol dioxygenases and Rieske dioxygenases) start with binding of O_2 at the metal complex, yielding the dioxygen-bound iron species shown in Fig. 2. When dioxygen binds to an iron(II) site, the resulting complex can be described by two extremes: Fe^{II}–O_2 or Fe^{III}–$O_2^{-\bullet}$. The metal coordination environment, which tunes the redox potential of iron, will determine which of the two formulas best describes the dioxygen-bound iron complex and which spin state characterizes its ground-state. It should be stressed here that the 2-His-1-carboxylate motif stabilizes the high-spin configuration on iron,[5,6] and the strong preference for the high-spin state on the metal distinguishes these iron active sites from the heme ones, where instead the high- and low-spin configurations are rather close in energy.[36] The low-spin configuration (singlet, $S = 0$) of the iron(II) complex coordinated by the 2-His-1-carboxylate motif and by three water molecules, lies about 12 kcal mol^{-1} higher in energy than the corresponding species with iron in the high-spin state (quintet, $S = 2$). After dioxygen binding, the high-spin configuration on iron is still more stable than the low-spin one by about 10 kcal mol^{-1}. Hence it is concluded that the non-heme 2-His-1-carboxylate environment does not support the low-spin electronic configuration on iron.

When dioxygen binds to the high-spin iron(II) site, different spin states of the resulting complex, such as the triplet ($S = 1$), the quintet ($S = 2$) and the septet ($S = 3$), arise from different spin coupling between the d-electrons of iron and the unpaired electron density on the O_2 moiety. In the septet and triplet spin states, the two unpaired electrons of O_2 are ferromagnetically or antiferromagnetically coupled with four unpaired d-electrons of the high-spin Fe^{II}. The formation of the quintet state involves an electron transfer from Fe^{II} to dioxygen and spin flip, since the electronic structure of this complex is best described as an iron(III)–superoxo species with one unpaired electron on the superoxide fragment antiferromagnetically coupled with the spins of the five unpaired electrons on Fe^{III}.

Considering the thermodynamics of O_2 trapping, the results from the calculations indicate that binding of dioxygen to the mononuclear iron(II) site is endergonic by at least 6 kcal mol^{-1}. This originates from a rather low enthalpic binding energy, usually calculated in the range of −3 to +6 kcal mol^{-1}, which does not compensate for the high entropic contribution ($-T\Delta S$) varying from 9 to 13 kcal mol^{-1}. Due to this endergonic nature of dioxygen binding to the mononuclear sites with the 2-His-1-carboxylate motif, the O_2-bound species are considered to be only short-lived intermediates along the reaction path.

It is important to note that the methodology employed to calculate the binding energy of O_2 seems to be accurate enough for this quite difficult task. Benchmark calculations performed for small iron complexes give credence to calculations employing the B3LYP functional. For example, the binding energy of dioxygen to $[Fe^{II}(OH)_2]$ on the septet potential energy surface has been calculated with the B3LYP method to be endothermic by 11.5 kcal mol^{-1}, while CCSD(T) calculations with an extensive basis set, 6–311+G(2d,2p), gave 12.0 kcal mol^{-1}. Similar agreement has been obtained for septet and quintet complexes between O_2 and $[Fe^{II}(H_2O)_3(HCOO)_2]$. The binding energies have been computed with B3LYP to be −0.7 and +2.5 kcal mol^{-1} for septet and quintet, respectively, while CASPT2 calculations gave +0.3 and +2.3 kcal mol^{-1} (in these calculations the ANO-S basis set was employed with the following contractions Fe: 6s4p3d1f, O and C: 3s2p1d, H: 2s1p; the active space consisted of five 3d orbitals on iron plus six valence orbitals of dioxygen accommodating 14 active electrons).

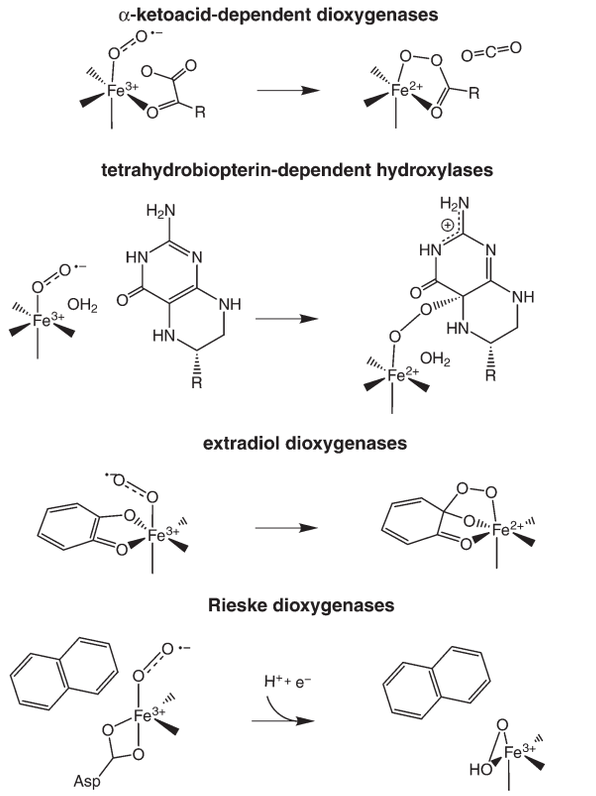

Fig. 2 The mechanisms for the initial step of O_2 activation in the four different enzymes.

Since nitric oxide (NO) is often used as surrogate for O_2, and it is known to bind to the Fe^{II} sites of clavaminic acid synthase (CAS)[37] and of naphthalene 1,2-dioxygenase, which is a Rieske-type dioxygenase,[38] it is interesting to compare the calculated binding energies of NO with those discussed above for O_2. The calculations indicate that the most stable adduct is formed in the quartet spin-state ($S = 3/2$) with a configuration best described as Fe^{II}–$NO^{\bullet}$. In the case of naphthalene dioxygenase, the NO enthalpic binding energy is 6.5 kcal mol^{-1}, while for the same model of the active site the O_2 enthalpic binding energy is only 0.5 kcal mol^{-1}. An even bigger difference is found for a model of the CAS active site. In this case, NO is bound by 8.8 kcal mol^{-1}, while the calculated energy gain for dioxygen trapping is only 0.9 kcal mol^{-1}. Thus, the experimental observations of nitrosyl adducts with the mononuclear non-heme iron sites are in fair agreement with the calculated NO binding energies, since, assuming that the error of the computational method is 3–5 kcal mol^{-1}, the calculated enthalpy can compensate for the entropy term (9–13 kcal mol^{-1}) due to NO trapping. However, the result for NO indicates that the binding energy is probably underestimated by a few kcal mol^{-1} and a similar effect for O_2 binding to Fe^{II} appears likely. It is in this context interesting to note that reducing the fraction of exact exchange from 20% to 15% increases the binding energy, also by a few kcal mol^{-1} in general. Improved results using 15% exact exchange is line with previous experience.[39]

Of the three possible spin states of the dioxygen-bound iron complex (*i.e.*, septet, triplet and quintet), the quintet species has been found to be the reactive form in the case of α-keto-acid-dependent dioxygenases, tetrahydrobiopterin-dependent hydroxylases and extradiol dioxygenases. Even though the quintet state is the least stable species among the three spin states, the quintet potential energy surface requires the lowest energetics for the chemical transformations of interest. This can be understood considering that full reduction of dioxygen requires four electrons and in these enzymes the reduction process occurs in two major steps; in each one of these steps, two electrons are supplied to the O_2 moiety. After dioxygen binding, the first two-electron reduction accomplished by pterin (cofactor) in tetrahydrobiopterin-dependent hydroxylases, or by the α-ketoacid (usually the co-substrate) in α-ketoacid-dependent dioxygenases or by catechol (substrate) in extradiol dioxygenases leads to the bridging-peroxide structures (*i.e.*, Fe^{II}–OO–R) shown in Fig. 2. Since in the ground state of this intermediate the ferrous ion is in a high-spin quintet state, it is the quintet species of the dioxygen-iron adduct that lies on the same potential energy surface as the product. Therefore, the quintet spin state provides the most direct route for the first two-electron reduction of O_2.

The $S = 2$ dioxygen-bound iron complex is usually best described as Fe^{III}–$O_2^{-\bullet}$. However, there exists another low-lying quintet state, which instead can be described as Fe^{II}–$O_2^{-\bullet}$ bound to a (co-)substrate radical, which is the actual reacting state. For the extradiol dioxygenase, this type of electronic distribution gives the lowest quintet state. Since the spins on dioxygen and the (co-)substrate have opposite directions in this state the formation of a bond is very easy, with a very low barrier once this state has been reached. A large part of the barrier for bridging-peroxide formation is therefore the excitation energy from the ground septet state of the dioxygen-bound complex to the tri-radical quintet state. In summary, it is thus expected that the quintet potential energy surface should involve the lowest barrier for the first step of dioxygen activation, which is indeed found to be the case in the calculations. Consistently, the septet and triplet species give rise to substantially higher barriers.

In the Rieske dioxygenases the dioxygen activation also follows the two-step pattern, though here the first two electrons are provided by the ferrous ion and an external source. Therefore, instead of the peroxo-bridged structure, the first intermediate is a high-spin iron(III) complex (sextet, $S = 5/2$) with a singly protonated peroxide bound to the metal in a side-on fashion.

After the first two-electron reduction of dioxygen yielding a peroxide species, the O–O bond is cleaved in different ways in the four families of enzymes, whose proposed mechanisms are presented in more details in separate subsections below. In the case of α-ketoacid-dependent dioxygenases and tetrahydrobiopterin-dependent hydroxylases, the following discussion focuses on the mechanism of formation of the activated oxygen species, that is, on the mechanism of oxidation of the ketoacid and of hydroxylation of pterin, respectively.

4 α-Ketoacid-dependent dioxygenases

The α-ketoacid-dependent dioxygenases form the largest family of mononuclear non-heme iron enzymes.[3,9,11–13] They are found in various types of organisms (*e.g.*, animals, plants, and bacteria), and are involved in a broad range of biochemical processes.[40] Besides the typical biosynthesis of primary and secondary metabolites, some enzymes from this family are involved in cellular oxygen sensing,[41,42] while others catalyze RNA and DNA dealkylation reaction, which is one of the strategies used by Nature for nucleic acid repair.[43–46]

In the catalytic reaction of α-ketoacid-dependent dioxygenases, the four-electron reduction of O_2 leads to the two-electron oxidative decarboxylation of the ketoacid and the two-electron oxidation of the substrate. In most cases the ketoacid is provided as a co-substrate (2-oxoglutarate also known as α-ketoglutarate), while in the subgroup of enzymes which are termed as internal ketoacid-dependent, the substrate has an in-built α-ketoacid functional group, and therefore, the α-ketoglutarate is not required.

Insights into the early stages of the catalytic cycle of these enzymes were obtained from kinetic, spectroscopy and X-ray crystallography results.[47–52] The keto-acid binds in the first coordination sphere of the metal after the displacement of two water ligands. A third water ligand is likely to be displaced upon binding of the substrate in the active site yielding a complex coordinated by the bidentate ketoacid and the 2-His-1-carboxylate motif. Strong experimental evidence stemming from studies on biomimetic complexes indicates that this five-coordinate complex binds dioxygen and forms a ferric–superoxo species, which is most probably involved in the decarboxylation reaction.[53,54] Despite the fact that α-ketoacid-dependent enzymes have received much scientific attention, experimental data considering the dioxygen activation steps following the O_2 binding are still scarce. Only very recently the product of the dioxygen activation has been spectroscopically characterized, and it has been shown that this catalytically relevant intermediate is a high-spin iron(IV) species with an iron–oxo core.[26–28]

In order to obtain deeper insights into the elusive mechanism of dioxygen activation performed by α-ketoacid-dependent dioxygenases the reaction between the five-coordinate species and dioxygen has been studied with hybrid DFT methods. In our investigations we have used two models for the active sites from the α-ketoacid family.[55,56] First, the dioxygen cleavage reaction has been studied for clavaminic acid synthase (CAS), for which high-resolution X-ray crystal structures are available,[52] and which is also a representative enzyme from the α-ketoglutarate-dependent group. Second, the full catalytic reaction of an internal ketoacid-dependent enzyme, namely, 4-hydroxyphenylpyruvate dioxygenase (4-HPPD), has been modeled. The reaction of a synthetic complex[57] mimicking the chemistry of α-ketoacid-dependent dioxygenases has also been examined with the same theoretical methods as those used in the enzyme studies, and it has been shown that the applied computational methodology is sufficiently accurate for proposing the most likely mechanism of the reaction studied.[58] The calculated energy profiles for the enzyme-catalyzed O_2 activation, derived for CAS and 4-HPPD, are similar, and therefore, only the results obtained for 4-HPPD are presented in Fig. 3, while the minor differences found for the two enzymes are discussed in the text.

Recent spectroscopic studies have demonstrated that the binary complex between 4-HPPD and its substrate (4-hydroxyphenylpyruvate also known as 4-HPP) is a mixture of species with five and six-coordinate active site iron.[59] Therefore, it follows that the reactive species, which has one vacancy in the iron coordination sphere, is available after substrate binding. For this reason, the sum of the energy of this species and free dioxygen has been used as a reference point in our calculations.

As discussed in the previous section, binding of dioxygen to the non-heme iron(II) complex has been computed to be slightly endothermic. More specifically, the septet ground state of the ternary complex (enzyme-substrate-O_2) lies 3.8 kcal mol^{-1} higher in energy than the reactants. Although the septet is the ground state for the dioxygen-bound complex, the computational results indicate that the lowest activation energy for the ketoacid decarboxylation involves the quintet potential energy surface (see discussion in section 3). For the septet and triplet spin states the calculated barriers are significantly higher. Therefore, once O_2 binds to iron, the catalytic cycle can continue provided that a spin-transition takes place. In order to address this phenomenon, the minimum energy point of the crossing between the non-interacting septet and quintet surfaces was optimized.[60] Quite interestingly, at the crossing point the geometry is very similar to the quintet complex, and therefore, the calculated energy is only slightly higher than that of the stable quintet intermediate

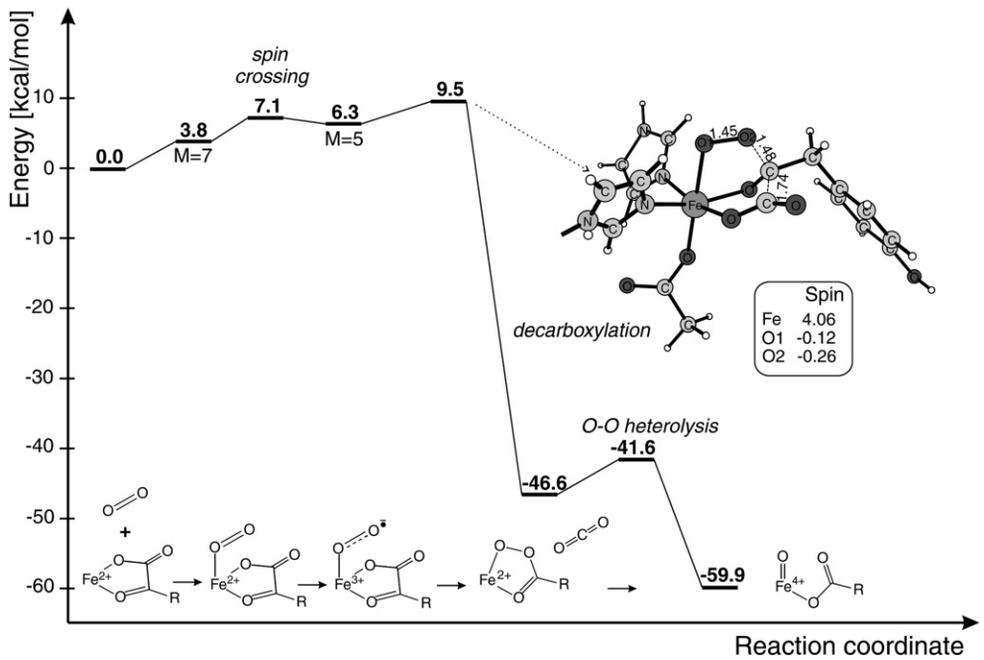

Fig. 3 Suggested mechanism for the O_2 activation in the α-ketoacid-dependent enzymes. Entropy is not included in the energies.

(7.1 *vs* 6.3 kcal mol^{-1}, Fig. 3). As a consequence, the activation energy for this spin transition is almost equal to the excitation energy from the septet to the quintet state, and this suggests a fast spin-transition due to the large spin–orbit coupling constant for iron.

The spin distribution calculated for the ternary quintet complex indicates that the electronic structure of this species corresponds to a high-spin iron(III) with bound superoxide. This electron transfer from iron to O_2 activates the complex for the following catalytic step, which may be interpreted as a nucleophilic attack of the iron(III)-superoxide species on the carbonyl carbon of the ketoacid. Indeed, for the optimized transition state for this reaction (Fig. 3), the spin distribution on the Fe–O_2 fragment still corresponds to the Fe^{III}–$O_2^{-\bullet}$ description, and therefore the attack on the ketoacid has been classified as a nucleophilic process. However, once the transition state is traversed, the CO_2 molecule is liberated, completing the two-electron reduction of O_2 and yielding the iron(II)-peracid intermediate. The computed activation energy is 9.5 kcal mol^{-1}, and as follows from the energy profile, it is also the rate-limiting barrier for the dioxygen activation reaction. Notably, the CO_2 molecule binds only very weakly to the ferrous ion, and therefore, it is concluded that the carbon dioxide is released from the active site immediately after it is produced. Consistent with this proposal, kinetic experiments indicate that CO_2 leaves the active site before the other products.[47] Finally, it can be noticed in Fig. 3 that the oxidative decarboxylation is very exothermic, and therefore, irreversible.

The complex produced in the decarboxylation reaction, namely, the iron(II)–peracid species, has been found to be very unstable toward O–O bond cleavage since the calculated activation energy for the O–O heterolysis is only 5 kcal mol^{-1}. Quite interestingly, the O–O bond heterolysis in CAS has been found to be a two-step process where two electrons are transferred from iron to the peracid O–O bond in two one-electron steps. The transfer of the second electron in CAS involves a very low activation barrier (*ca.* 1 kcal mol^{-1}), which vanishes completely for 4-HPPD. The reason for this minor difference could be the slightly different arrangement of ligands around iron. More specifically, in the case of CAS, dioxygen binds *trans* to a histidine ligand, while in 4-HPPD it occupies a position opposite to the carboxylate group of glutamate.

The final product of dioxygen activation is the high-spin iron(IV)–oxo species which is responsible for various oxidative reactions catalyzed by α-ketoacid dependent enzymes. The electronic structure of this species is very similar to the bonding situation in triplet dioxygen.[61] The Fe–O bond, which has formally a double-bond character, originates from distributing eight electrons on six molecular orbitals of the FeO fragment (σ,π and π*). The fact that the two π* levels are singly occupied causes the oxo ligand to have a significant spin population (around 0.7), while the other two unpaired electrons occupy the non-bonding orbitals of iron ($d_{x^2-y^2}$ and d_{xy}). Notably, the calculated Fe–O distance for the ferryl–oxo species (1.66 Å) is in good agreement with the available experimental structure for a synthetic complex.[24]

5 Tetrahydrobiopterin-dependent hydroxylases

Phenylalanine hydroxylase (PAH), tyrosine hydroxylase (TyrH) and tryptophan hydroxylase (TrpH), also known as tetrahydrobiopterin-dependent hydroxylases, employ molecular oxygen and the pterin cofactor (BH_4) to carry out hydroxylation of the side chains of the aromatic amino acids.[14–16] In mammals, they play a key role in the catabolism of amino acids (PAH) and in the synthesis of neurotransmitters and hormones (TyrH and TrpH).

The catalytic cycle can be viewed as occurring in two steps: dioxygen activation associated with hydroxylation of the cofactor (B of Fig. 1) followed by the hydroxylation of the aromatic ring. The cofactor supplies two of the four electrons required to fully reduce O_2, while the other two electrons are provided by the aromatic amino acid. The high sequential and structural homology of PAH, TyrH, and TrpH suggests that these three hydroxylases share a similar catalytic mechanism,[62] which has to account for the experimental observation that the oxygen atom of the hydroxylated cofactor and the oxygen atom of the hydroxylated amino acid originate from molecular oxygen.[63,64]

The theoretical investigation of pterin hydroxylation led us to propose the reaction mechanism for dioxygen activation that is summarized in Fig. 4.[65] The quantum chemical model that was employed for these calculations was taken from the crystal structure of the binary complex of PAH with the cofactor,[66] and is displayed in the same figure, which shows that the pterin cofactor binds in the second coordination sphere of the metal complex. An iron(II)–peroxy–pterin intermediate is initially generated through the formation of a new C–O bond,

following the attack of the dioxygen-bound iron complex to the 4a position of the cofactor. The corresponding transition state structure is shown in Fig. 4. In this step, which implies a two-electron reduction of dioxygen by pterin, iron does not carry out any redox activity but only stabilizes the developing charge on the nascent peroxo group. Once the peroxide is formed, the subsequent steps involve the O–O bond heterolysis promoted by one of the water ligands, which donates a proton to the distal oxygen yielding the hydroxylated cofactor and HO–Fe^{IV}=O. Similarly to the cleavage discussed in α-ketoacid-dependent dioxygenases, the O–O bond heterolysis occurs in two one-electron steps. Pterin hydroxylation leads to the formation of activated oxygen, namely, the high-valent iron–oxo intermediate, which is then capable of aromatic hydroxylation through an electrophilic attack on the ring of the aromatic amino acids.[67]

As anticipated above, the cofactor hydroxylation process occurs along the quintet potential energy surface, which is an excited state of the Fe^{II}–O_2 reactant, but which is the ground state of the iron(II)–peroxy–pterin intermediate. The ground state of the dioxygen complex is instead the septet and, as discussed previously, the septet to quintet transition should require a quite low energy barrier. The energy diagram reported in Fig. 4 shows that the C–O bond formation is rate-limiting during the cofactor hydroxylation process, and this means that the slow step arises from the two-electron reduction of O_2 forming a peroxide. It should be mentioned that, while scanning the potential energy surface joining the reactant and the first stable intermediate, a metastable species interpreted as a cationic pterin radical coupled to an iron(II)–superoxo complex was optimized, and found to lie 7–8 kcal mol^{-1} higher in energy than the reactant. This structure originating from the one-electron reduction of O_2 by the cofactor was highly unstable, and could be formed without any significant additional activation energy. In order to probe whether O_2 might react with BH_4 without assistance from iron, dioxygen was also placed in the second coordination sphere of the metal, but the wave function corresponding to the pterin-radical-cation/superoxide couple was never obtained. In the proposed mechanism of Fig. 4, iron plays an essential role in catalysis providing the required electrostatic stabilization of the negative charge developing on dioxygen during the C–O bond formation. We were not able to locate a positively charged residue in the active site pocket of these enzymes that could perform an analogous task.

The theoretical modeling of pterin hydroxylation predicts a barrier of 16.7 kcal mol^{-1} with respect to the dioxygen-bound iron complex, and this barrier increases roughly by 10 kcal mol^{-1} when the entropic contribution associated with binding of O_2 is included. More recent calculations with a bigger model that was derived from the crystal structure of PAH binding both the cofactor and a substrate analogue,[68,69] led to a lower barrier for the C–O bond formation.[70] According to the experimental structure of the ternary complex, fewer water molecules are present in the new model, which included only one water ligand and no water mediating the interaction between the pterin and the carboxylate group of a glutamate residue. While the thermodynamics for dioxygen binding was not significantly affected by the new structural arrangement, the iron(II)–peroxy–pterin intermediate could be formed with an energy barrier which is about 5 kcal mol^{-1} lower than the corresponding value obtained in our first study. The new model indicates that the activation barrier for the two-electron reduction of dioxygen is affected by a different structural organization around the cofactor, and more specifically by the carboxylate group of Glu286, which is likely to stabilize the positive charge delocalized in the pyrimidine ring of the peroxy–pterin intermediate.

Tetrahydrobiopterin-dependent hydroxylases share many similarities with the α-ketoacid-dependent dioxygenases. Both enzymes activate dioxygen through the formation of a high-valent iron–oxo species. Moreover, in both cases, the rate determining step for the formation of the high-valent iron–oxo species is not the O–O bond heterolysis, but the two-electron reduction of O_2 yielding an Fe^{II}–OOR species (the peracid for α-ketoacid-dependent enzymes and the peroxide in tetrahydrobiopterin-dependent enzymes). Interestingly, the two computed barriers associated with the rate-limiting step in the two enzymes are quite similar, even though the thermodynamics of the two corresponding steps is very different. Formation of the pterin-peroxide is found endothermic by 7.4 kcal mol^{-1}, while formation of the peracid, which is coupled to decarboxylation of the ketoacid, is highly exothermic (−46.7 kcal mol^{-1}). Furthermore, the full process of dioxygen activation generating Fe^{IV}=O is exothermic by only 8.9 kcal mol^{-1} for the aromatic amino acid hydroxylases compared to a calculated exothermicity of 59.9 kcal mol^{-1} for the α-ketoacid-dependent enzymes.

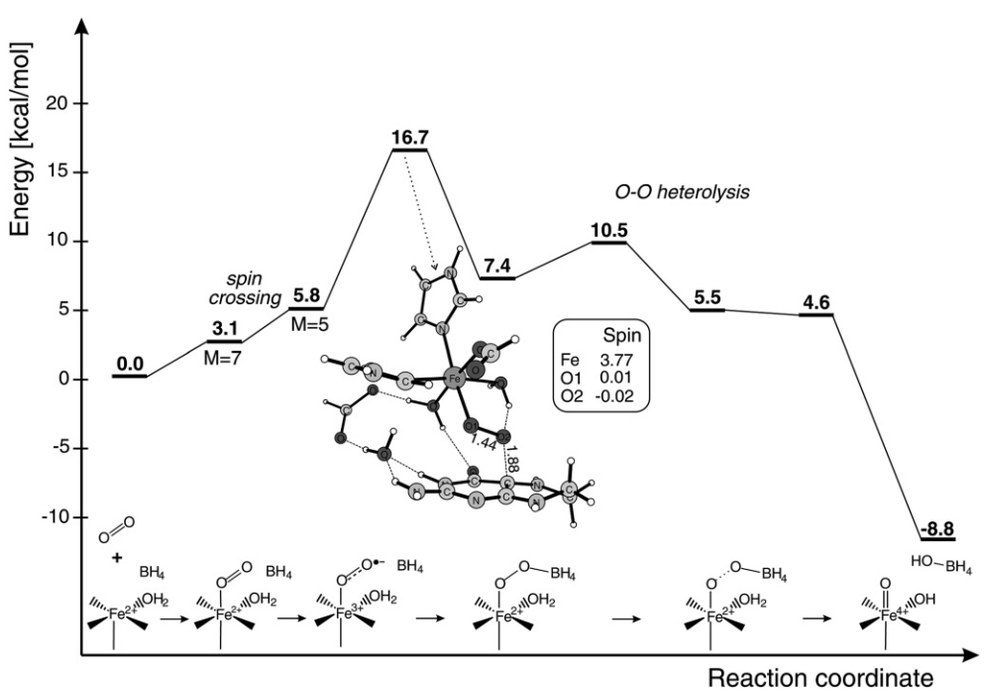

Fig. 4 Suggested mechanism for tetrahydrobiopterin-dependent hydroxylases. Entropy is not included in the energies.

6 Extradiol dioxygenases

The extradiol dioxygenases are enzymes that with the help of dioxygen cleave the C–C bond adjacent to the hydroxyl groups of catecholic substrates, producing 2-hydroxymuconaldehyde acids. This family of enzymes plays an important environmental role by facilitating microbial aerobic degradation of catechol and substituted catechol substrates,[18] and they have received a large attention since they were discovered by Dagley and Stopher[17] in the 1950s.

Several high-resolution X-ray structures of extradiol dioxygenases have been determined. For the present modeling a structure with a bound catechol substrate was used as a starting point.[71] The coordination around the ferrous center is octahedral with two histidines, a glutamate, and one water molecule. The catechol fills the two remaining coordination sites. Concerning the water ligand, it should be noted that the occupation of this position is only partial.

Based on available spectroscopic and X-ray crystallographic data, several mechanisms of how the extradiol dioxygenases operate have been suggested, for example by Lipscomb and Que[72,73] and by Bugg and coworkers.[18,74–76] There is one earlier quantum chemical study by Deeth and Bugg.[77] An intriguing question in the context of the mechanism of extradiol dioxygenases is how these enzymes selectively catalyze the ring-fission.

In the quantum chemical model used to study the mechanism of extradiol dioxygenases,[78] experimentally known structural features were built in, such as the known position of the catechol substrate and the experimentally suggested position for dioxygen. The amino acids at the active site implied to be most significant for the substrate mechanism, have been included in the model. Apart from the residues in the first coordination shell mentioned above, two histidines, one aspartate and one tyrosine (modeled by water) in the second shell were also included in the model, see Fig. 5.

The first part of the suggested mechanism is shown in Fig. 5. The mechanism starts by the binding of the substrate to the ferrous reactant. The catechol substrate is found to be bound as a mono-anion, in agreement with experimental evidence.[71,72,79] One proton of the catechol has moved to a second shell histidine. In the next step dioxygen binds to iron, as described in general terms in section 3 above. In detail, dioxygen replaces the water ligand which moves to the second shell in between the peroxy ligand and a second shell aspartate. Simultaneously, the second catechol proton moves to the same aspartate. The hydrogen bonds formed are important since dioxygen becomes anionic. For the septet state the enthalpic binding energy is 3.4 kcal mol^{-1}. With an entropy loss of 9–13 kcal mol^{-1}, the binding of dioxygen becomes endergonic as for the other enzymes described here. From the septet state a spin-crossing is required to reach the reactive ferrous quintet state (see discussion in section 3). This crossing should occur easily since the structures of the septet and quintet states are quite similar and they are close in energy, like for α-ketoacid-dependent enzymes discussed above. The quintet dioxygen-bound state, which is 5.5 kcal mol^{-1} higher in energy than the septet, is perfectly suited for formation of the bridging-peroxide bond since there is a spin on the substrate of the opposite direction to the spin on the peroxy radical. The barrier for peroxide formation is consequently very low with only 3.0 kcal mol^{-1} once the active quintet dioxygen state has been formed. Overall, bridging-peroxide formation is weakly endothermic by 1.1 kcal mol^{-1} counted from the septet dioxygen adduct.

After the peroxide has been formed, the rate-limiting O–O bond cleavage occurs. The optimized transition state structure is shown in Fig. 5. As shown in there, the peroxide has been protonated by the proton from the second shell aspartate. This protonation, which occurs concertedly with the O–O bond cleavage, is very important for keeping the barrier low. The transition state is one of an essentially homolytic cleavage, as noticed by an increasing spin-population on the oxygen on the substrate side. The proton on the other oxygen is important for attracting an electron from the ferrous iron to this oxygen. The barrier for O–O bond cleavage is 13.9 kcal mol^{-1} with respect to the peroxide precursor. This reaction step is endothermic by 8.4 kcal mol^{-1} and leads to a ferric complex and an oxy-substrate with substantial radical character.

The precise nature of the oxy-substrate intermediate turns out to be very important for the selectivity of the following C–C bond cleavage of the catechol. Some calculations on the oxy-substrate alone are indicative of what factors are important for the selectivity. It turns out that a formation of a pure oxy-substrate radical will lead to a spontaneous cleavage of the bond in between (intra) the hydroxyls of the catechol, which is

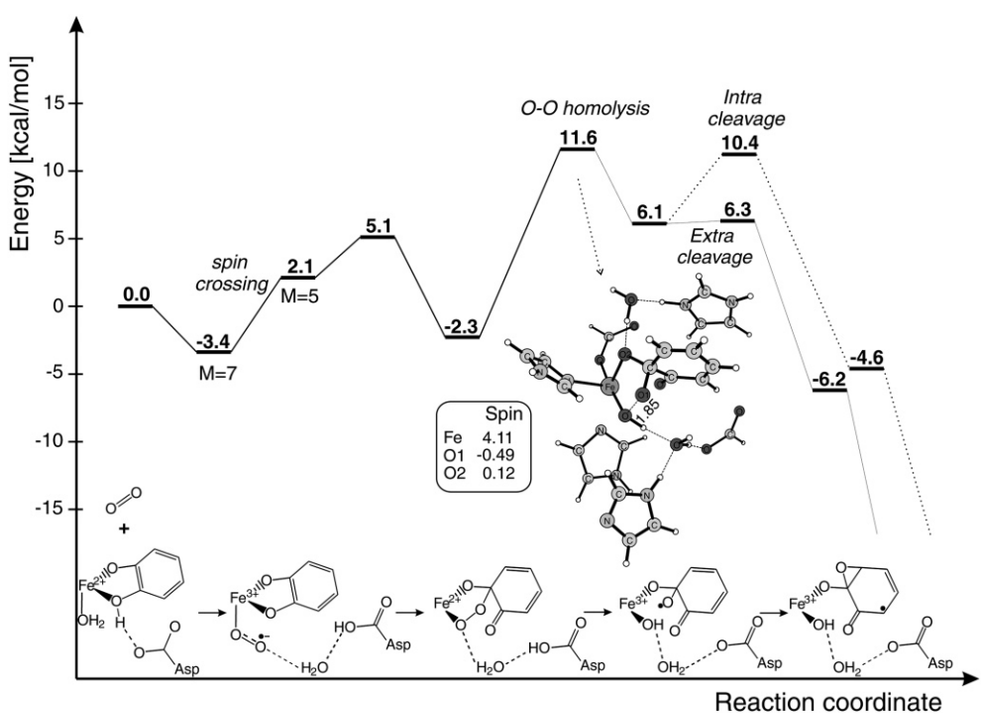

Fig. 5 Suggested mechanism for extradiol dioxygenases. Entropy is not included in the energies.

not the desired cleavage. On the other hand, the formation of a pure oxy-substrate anion will preferentially lead to an epoxide with the oxygen between the carbons where the bond should be broken. However, to cleave this (extra) C–C bond requires a substantial barrier for the oxy-anion substrate. The enzyme has therefore found an optimal compromise with formation of an oxy-substrate that has about equal amounts of radical and anionic character. This leads to an essentially barrierless formation of the extra epoxide. In contrast, a cleavage of the intra C–C bond occurs with a calculated barrier of 4.3 kcal mol^{-1}. This barrier difference is thus suggested to explain the selectivity of the enzyme. Once the extra epoxide is formed, the substrate will adopt a pure radical character and the extra C–C bond will be cleaved with almost no barrier. The reaction will therefore selectively follow the extra-cleavage pathway as desired. In a parallel study of the mechanism for intradiol dioxygenases, O–O bond cleavage instead leads to a pure oxy-substrate radical, which in turn will lead to a barrierless intra-diol cleavage.[80] It is clear that a selectivity that depends on just the character of an intermediate can be quite sensitive. In line with this expectation, the model studies showed that the selectivity of the extradiol enzyme can be modified in different ways by changes of the active site. For example, when the protonated second shell histidine was removed from the model, the polarization of the active site was changed to an extent that a more radical substrate was obtained which led to a preference for intradiol cleavage instead. The high sensitivity of the selectivity is in line with results from mutation studies[81] and biomimetic studies.[74,82]

Which of the two oxygens of the bridging peroxide that becomes protonated is very important for the subsequent chemistry. It is in this context interesting to compare the O–O bond cleavage of the bridging peroxide to the one discussed above for pterin-dependent hydroxylases (see Fig. 6). In that case a protonation of the oxygen bound to the cofactor is sterically forced by having a water molecule coordinated to iron as proton donor, and instead leads to the formation of an Fe^{IV}=O species. In the extradiol dioxygenases the protonation is not sterically dictated. Instead, the most negative oxygen becomes protonated. With charges of the oxygens of the bridging-peroxide precursor of −0.50 for the oxygen bound to iron and a charge of only −0.28 on the oxygen bound to the substrate, the energetic preference for hydrogen bonding to the iron bound oxygen is actually higher by more than 10 kcal mol^{-1}. This charge difference between the oxygen thus prevents the formation of the undesired Fe^{IV}=O species for the extradiol dioxygenases. The cleavage of the O–O bond is not driven by the stability of the product. In fact, the Fe^{IV}=O product is 2.5 kcal mol^{-1} more stable than the ferric-oxyradical product on the preferred pathway. It is furthermore interesting to note that the charge difference between the oxygens of the bridging peroxide in the pterin-dependent enzyme is much smaller, with charges of −0.44 and −0.34, respectively. The reason for this difference between the enzymes is that the cofactor in the pterin-dependent enzyme is positively charged and therefore polarizes the negative charge on the peroxide in the direction of the cofactor.

The steps following the cleavage of the extradiol C–C bond are quite complicated and less interesting from a general chemical perspective, and will therefore be only briefly described here. The C–C bond cleavage will first lead to a seven-membered ring, in a quite exothermic step of 28 kcal mol^{-1}. The hydroxyl ligand on the ferric iron will then attack the radical carbon of one of the substrate carbonyl groups. This step is exothermic by 25 kcal mol^{-1}. After a few proton transfers the seven-membered ring will be cleaved between the oxygen and a carbon. After some rearrangements the final 2-hydroxymuconaldehyde acid product is formed, also in a rather exothermic step of 17 kcal mol^{-1}. All the final steps have very low barriers.

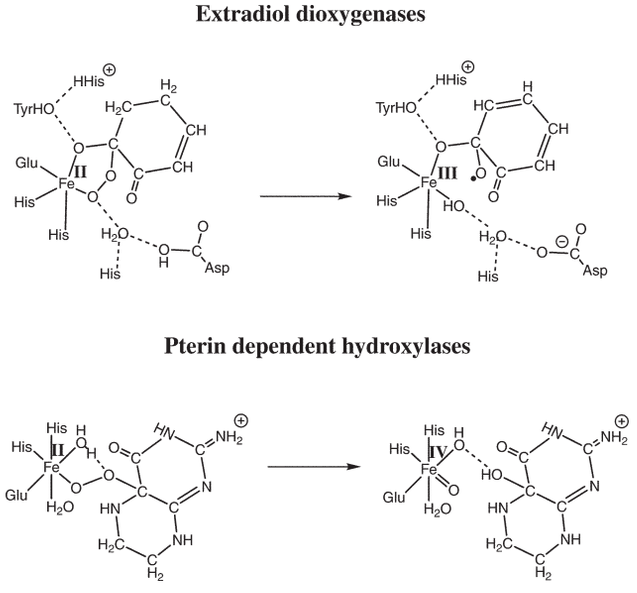

Fig. 6 O–O Bond cleavage in extradiol dioxygenases and pterin-dependent hydroxylases.

7 Rieske dioxygenases

Rieske non-heme iron dioxygenases are bacterial enzymes that initiate the degradation of aromatic hydrocarbons, yielding the corresponding *cis*-dihydrodiols;[19,20] the diols are subsequently degraded by the intra- and extra-diol oxygenases. The best studied Rieske dioxygenase is naphthalene 1,2-dioxygenenase (D of Fig. 1), where full reduction of O_2 is achieved employing two electrons from naphthalene and two more electrons from an external source, nicotinamide adenine nucleotide (NADH). Naphthalene 1,2-dioxygenase is a three-component enzyme, which accommodates a mononuclear non-heme iron(II) center in the catalytic domain located in the oxygenase component, where a Rieske [2Fe–2S] cluster is also hosted.[22,83] The other two components of the enzyme, the reductase and the ferredoxin components, provide the electron transfer pathway, through which the two external electrons reach the active site.

Calculations with a model including both the mononuclear and the Rieske centers,[84] indicate that binding of molecular oxygen to iron(II) coupled with the transfer of one external electron (*i.e.*, the transfer of one electron from the reduced Rieske cluster to the mononuclear complex) is exothermic by 9.9 kcal mol^{-1}. If the reaction is decomposed into two subsequent steps, namely the dioxygen binding and the electron transfer steps, the computed exothermicity can be partitioned into two energy contributions. The first contribution is associated with the enthalpic energy change for O_2 binding to iron(II), which similarly to the tetrahydrobiopterin- and α-ketoacid-dependent enzymes is close to zero. The second contribution arises from the difference between the ionization potential (IP) of the reduced Rieske cluster and the electron affinity (EA) of the dioxygen-bound iron(II) complex.

A free energy change for the initial dioxygen activation process can be obtained assuming that the only significant contribution to the entropic term originates from the binding of O_2 to Fe^{II}. The overall process leading to an iron(II)–superoxo (iron(III)–peroxo) species then becomes slightly endergonic (ΔG = 1.1 kcal mol^{-1}, $-T\Delta S$ = 11.0 kcal mol^{-1}). The computed free energy change of only 1 kcal mol^{-1} together with the estimate of a low activation barrier for the electron transfer process seems to indicate that the first step of dioxygen activation in naphthalene dioxygenase is a reversible equilibrium, that can be finely shifted toward the reactant or the product sides by an appropriate protein environment. Furthermore, it can also be concluded that O_2 triggers the electron transfer from the reduced Rieske cluster.

Since it has been observed that naphthalene *cis*-dihydroxylation occurs in single turnover also when only one external electron is available (*i.e.*, the electron from the reduced Rieske cluster),[23] an iron(III)-(hydro)peroxide itself should be capable of

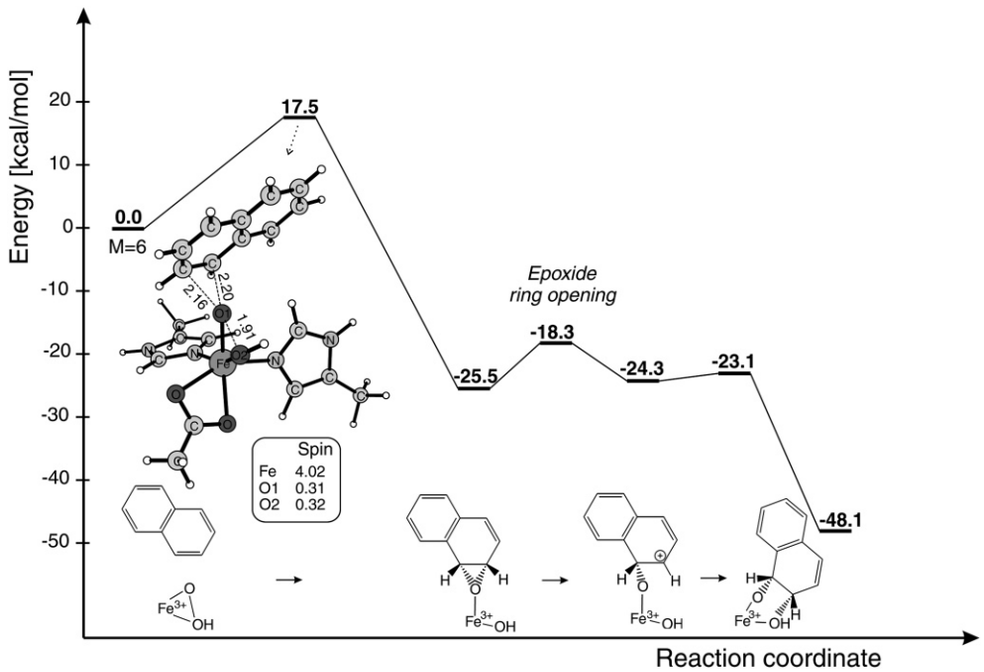

Fig. 7 Suggested mechanism for Rieske dioxygenases. Entropy is not included in the energies.

oxidation of the substrate. The X-ray data of the iron complex with O_2 binding in a side-on fashion[21] have been used to model the *cis*-dihydroxylation reaction in naphthalene 1,2-dioxygenase. The theoretical investigations indicate that dioxygenation of the substrate may be obtained from the attack of an iron(III)-hydroperoxo species at the aromatic ring.[85] The energetics associated with the protonation of the ferric–peroxide were not investigated because detailed structural information on the proton source were not available.

The proposed *cis*-dihydroxylation mechanism by the high-spin Fe^{III}–OOH species is illustrated in Fig. 7 and it implicates a concerted step, where the O–O bond is cleaved concomitantly with the formation of an epoxide, that is, the formation of two C–O bonds. The epoxide then converts into a carbocation, and subsequently into the observed product (the diol) with a very low activation energy. It should be observed that the cationic intermediate resembles the arenium-cation species previously proposed in the catalytic cycle of aromatic amino acid hydroxylases and, similarly, it might easily undergo a NIH shift yielding, however, an undetected product. The diol formation leads to an iron(III) center, which can be reduced to the initial ferrous oxidation state by a second external electron from NADH.[23]

A pathway involving a high-valent iron–oxo species (*i.e.*, HO–Fe^{V}=O) has also been examined but it was excluded because it involves too high an activation barrier for the O–O bond cleavage. Interestingly, compelling experimental evidence supports the involvement of an analogous HO–Fe^{V}=O species in the *cis*-dihydroxylation reaction catalyzed by synthetic non-heme iron complexes,[86–88] a mechanism which has been confirmed by theoretical studies on the same catalyst.[89]

8 Summary and conclusions

The catalytic mechanisms of four families of non-heme iron enzymes characterized by the 2-His-1-carboxylate coordination environment have been discussed with major attention on the dioxygen activation process. A comparison among the mechanisms proposed for these enzymes show that all of them involve the formation of a dioxygen-bound iron(II) complex. This first step is endergonic because the low enthalpic binding energy of O_2 to Fe^{II} does not balance the corresponding entropy loss. Once the adduct is formed, O_2 undergoes a two-electron reduction, which leads to a bridging-peroxide species (Fe^{II}–OOR) in the cases of α-ketoacid-dependent dioxygenases, tetrahydrobiopterin-dependent hydroxylases, and extradiol dioxygenases. For these three families, the reducing equivalents required are provided by external organic molecules: the ketoacid, which is usually the co-substrate in α-ketoacid-dependent oxygenases, the pterin cofactor in tetrahydrobiopterin-dependent hydroxylases, and the catechol substrate in the extradiol dioxygenases. In Rieske dioxygenases, and more specifically in naphthalene 1,2-dioxygenase, only one electron is supplied by an external source in the first step of dioxygen activation, which leads to an iron(III)-peroxide species, while the second electron is provided by iron of the mononuclear non-heme center. The peroxide species, which is formed in the four enzymes, then undergoes O–O bond cleavage. The α-ketoacid-dependent dioxygenases and tetrahydrobiopterin-dependent hydroxylases follow a similar catalytic pathway for this step, in contrast to the different strategy adopted by the other two families, extradiol and Rieske dioxygenases. While catalysis of the former families involves an initial formation of a high-spin iron–oxo species, Fe^{IV}=O (see Figs. 3 and 4), which subsequently performs oxidation of the substrate, the latter carry out the O–O bond cleavage concomitantly with the oxidation of the substrate (see Figs. 5 and 7). It can be noted, that in the case of α-ketoacid-dependent dioxygenases and tetrahydrobiopterin-dependent hydroxylases, iron functions as a transient reducing agent along the reaction pathway, providing the required two reducing equivalents for the oxo group in the Fe^{IV}=O intermediate obtained after O–O bond heterolysis. In extradiol dioxygenase the O–O bond cleavage is mainly homolytic leading to a ferric complex and an oxy-substrate species with substantial radical character. The precise character of this species is found to dictate the subsequent selective extradiol cleavage. The hydrogen bonding to the iron bound oxygen of the bridging peroxide is found to be an essential part of the mechanism preventing formation of an undesired Fe(IV)=O species.

References

1 *Handbook of Metalloproteins*, ed. I. Bertini, A. Sigel and H. Sigel, Marcel Dekker, Inc, New York, 2001.
2 *Handbook of Metalloproteins*, ed. A. Messerschmidt, R. Huber, T. Poulos and K. Wieghardt, John Wiley & Sons, Chichester, 2001.
3 E. I. Solomon, T. C. Brunold, M. I. Davis, J. N. Kemsley, S. K. Lee, N. Lehnert, F. Neese, A. J. Skulan, Y. S. Yang and J. Zhou, *Chem. Rev.*, 2000, **100**, 235.
4 M. Sono, M. P. Roach, E. D. Coulter and J. H. Dawson, *Chem. Rev.*, 1996, **96**, 2841.
5 E. I. Solomon, *Inorg. Chem.*, 2001, **40**, 3656.

6 E. I. Solomon, A. Decker and N. Lehnert, *Proc. Natl. Acad. Sci. USA*, 2003, **100**, 3589.
7 R. H. Holm, P. Kennepohl and E. I. Solomon, *Chem. Rev.*, 1996, **96**, 2239.
8 L. Que, Jr., *Nat. Struct. Biol.*, 2000, **7**, 182.
9 M. Costas, M. P. Mehn, M. P. Jensen and L. Que, Jr., *Chem. Rev.*, 2004, **104**, 939.
10 L. Que, Jr. and R. Y. N. Ho, *Chem. Rev.*, 1996, **96**, 2607.
11 T. D. H. Bugg, *Tetrahedron*, 2003, **59**, 7075.
12 C. J. Schofield and Z. Zhang, *Curr. Opin. Struct. Biol.*, 1999, **9**, 722.
13 M. J. Ryle and R. P. Hausinger, *Curr. Opin. Chem. Biol.*, 2002, **6**, 193.
14 T. J. Kappock and J. P. Caradonna, *Chem. Rev.*, 1996, **96**, 2659.
15 T. Flatmark and R. C. Stevens, *Chem. Rev.*, 1999, **99**, 2137.
16 P. F. Fitzpatrick, *Biochemistry*, 2003, **42**, 14083.
17 S. Dagley and D. Stopher, *Biochem. J.*, 1959, **73**, 16.
18 T. D. H. Bugg and C. Winfield, *Nat. Prod. Rep.*, 1998, **15**, 513.
19 D. T. Gibson and R. E. Parales, *Curr. Opin. Biotechnol.*, 2000, **11**, 235.
20 R. E. Parales, *J. Ind. Microbiol. Biotechnol.*, 2003, **30**, 271.
21 A. Karlsson, J. V. Parales, R. E. Parales, D. T. Gibson, H. Eklund and S. Ramaswamy, *Science*, 2003, **299**, 1039.
22 B. Kauppi, K. Lee, E. Carredano, R. E. Parales, D. T. Gibson, H. Eklund and S. Ramaswamy, *Structure*, 1998, **6**, 571.
23 M. D. Wolfe, J. V. Parales, D. T. Gibson and J. D. Lipscomb, *J. Biol. Chem.*, 2001, **276**, 1945.
24 J. U. Rohde, J. H. In, M. H. Lim, W. W. Brennessel, M. R. Bukowski, A. Stubna, E. Münck, W. Nam and L. Que, Jr., *Science*, 2003, **299**, 1037.
25 M. H. Lim, J.-U. Rohde, A. Stubna, M. R. Bukowski, M. Costas, R. Y. H. Ho, E. Műnck, W. Nam and L. Que, Jr., *Proc. Natl. Acad. Sci. USA*, 2003, **100**, 3665.
26 J. C. Price, E. W. Barr, B. Tirupati, J. M. Bollinger, Jr. and C. Krebs, *Biochemistry*, 2003, **42**, 7497.
27 J. C. Price, E. W. Barr, T. E. Glass, C. Krebs and J. M. Bollinger, Jr., *J. Am. Chem. Soc.*, 2003, **125**, 13008.
28 D. A. Proshlyakov, T. F. Henshaw, G. R. Monterosso, M. J. Ryle and R. P. Hausinger, *J. Am. Chem. Soc.*, 2004, **126**, 1022.
29 A. D. J. Becke, *Chem. Phys.*, 1993, **98**, 5648.
30 C. Lee, W. Yang and R. G. Parr, *Phys. Rev. B: Condens. Matter*, 1988, **37**, 785.
31 P. J. Stevens, F. J. Devlin, C. F. Chablowski and M. J. Frisch, *J. Phys. Chem.*, 1994, **98**, 11623.
32 M. J. Frisch, G. W. Trucks, H. B. Schlegel, G. E. Scuseria, M. A. Robb, J. R. Cheeseman, J. A. Montgomery, Jr., T. Vreven, K. N. Kudin, J. C. Burant, J. M. Millam, S. S. Iyengar, J. Tomasi, V. Barone, B. Mennucci, M. Cossi, G. Scalmani, N. Rega, G. A. Petersson, H. Nakatsuji, M. Hada, M. Ehara, K. Toyota, R. Fukuda, J. Hasegawa, M. Ishida, T. Nakajima, Y. Honda, O. Kitao, H. Nakai, M. Klene, X. Li, J. E. Knox, H. P. Hratchian, J. B. Cross, C. Adamo, J. Jaramillo, R. Gomperts, R. E. Stratmann, O. Yazyev, A. J. Austin, R. Cammi, C. Pomelli, J. W. Ochterski, P. Y. Ayala, K. Morokuma, G. A. Voth, P. Salvador, J. J. Dannenberg, V. G. Zakrzewski, S. Dapprich, A. D. Daniels, M. C. Strain, O. Farkas, D. K. Malick, A. D. Rabuck, K. Raghavachari, J. B. Foresman, J. V. Ortiz, Q. Cui, A. G. Baboul, S. Clifford, J. Cioslowski, B. B. Stefanov, G. Liu, A. Liashenko, P. Piskorz, I. Komaromi, R. L. Martin, D. J. Fox, T. Keith, M. A. Al-Laham, C. Y. Peng, A. Nanayakkara, M. Challacombe, P. M. W. Gill, B. Johnson, W. Chen, M. W. Wong, C. Gonzalez and J. A. Pople, *GAUSSIAN03*, Gaussian, Inc., Pittsburgh, PA, 2003.
33 Schrödinger, Inc., Portland, Oregon, *JAGUAR 4.0/4.1/4.2*, 2000.
34 D. J. Tannor, B. Marten, R. Murphy, R. A. Friesner, D. Sitkoff, A. Nicholls, M. Ringnalda, W. A. Goddard III and B. Honig, *J. Am. Chem. Soc.*, 1994, **116**, 11875.
35 B. Marten, K. Kim, C. Cortis, R. A. Friesner, R. Murphy, M. Ringnalda, D. Sitkoff and B. Honig, *J. Phys. Chem.*, 1996, **100**, 11775.
36 K. P. Jensen and U. Ryde, *J. Biol. Chem.*, 2004, **279**, 14561.
37 Z. Zhang, J. Ren, K. Harlos, C. H. McKinnon, I. J. Clifton and C. J. Schofield, *FEBS Lett.*, 2002, **517**, 7.
38 A. Karlsson, Ph.D. thesis, Swedish University of Agricultural Science, Uppsala, 2002.
39 M. Reiher, O. Salomon and B. A. Hess, *Theor. Chem. Acc.*, 2001, **107**, 48.
40 A. G. Prescott and M. D. Lloyd, *Nat. Prod. Rep.*, 2000, **17**, 367.
41 M. Ivan, K. Kondo, H. Yang, W. Kim, J. Valiando, M. Ohh, A. Salic, J. M. Asara, W. S. Lane and W. G. Kaelin, Jr., *Science*, 2001, **292**, 464.
42 P. Jaakkola, D. R. Mole, Y. M. Tian, M. I. Wilson, J. Gielbert, S. J. Gaskell, A. von Kriegsheim, H. F. Hebestreit, M. Mukherji, C. J. Schofield, P. H. Maxwell, C. W. Pugh and P. J. Ratcliffe, *Science*, 2001, **292**, 468.
43 S. C. Trewick, T. F. Henshaw, R. P. Hausinger, T. Lindahl and B. Sedgwick, *Nature*, 2002, **419**, 174.
44 P. O. Falnes, R. F. Johansen and E. Seeberg, *Nature*, 2002, **419**, 178.
45 P. A. Aas, M. Otterlei, P. O. Falnes, C. B. Vågbø, F. Skorpen, M. Akbari, O. Sundheim, M. Bjørås, G. Slupphaug, E. Seeberg and H. E. Krokan, *Nature*, 2003, **421**, 859.
46 B. Sedgwick, *Nat. Rev. Mol. Cell. Biol.*, 2004, **5**, 148.
47 E. Holme, *Biochemistry*, 1975, **22**, 4999.
48 M. J. Ryle, R. Padmakumar and R. P. Hausinger, *Biochemistry*, 1999, **38**, 15278.
49 E. G. Pavel, J. Zhou, R. W. Busby, M. Gunsior, C. A. Townsend and E. I. Solomon, *J. Am. Chem. Soc.*, 1998, **120**, 743.
50 J. Zhou, M. Gunsior, B. O. Bachmann, C. A. Townsend and E. I. Solomon, *J. Am. Chem. Soc.*, 1998, **120**, 13539.
51 J. Zhou, W. L. Kelly, B. O. Bachmann, M. Gunsior, C. A. Townsend and E. I. Solomon, *J. Am. Chem. Soc.*, 2001, **123**, 7388.
52 Z. Zhang, J. Ren, D. K. Stammers, J. E. Baldwin, K. Harlos and C. J. Schofield, *Nature. Struct. Biol.*, 2000, **7**, 127.
53 Y. M. Chiou and L. Que, Jr., *J. Am. Chem. Soc.*, 1995, **117**, 3999.
54 E. H. Ha, R. Y. N. Ho, J. F. Kisiel and J. S. Valentine, *Inorg. Chem.*, 1995, **34**, 2265.
55 T. Borowski, A. Bassan and P. E. M. Siegbahn, *Chem. Eur. J.*, 2004, **10**, 1031.
56 T. Borowski, A. Bassan and P. E. M. Siegbahn, *Biochemistry*, 2004, **43**, in press.
57 M. P. Mehn, K. Fujisawa, E. L. Hegg and L. Que, Jr., *J. Am. Chem. Soc.*, 2003, **125**, 7828.
58 T. Borowski, A. Bassan and P. E. M. Siegbahn, *Inorg. Chem.*, 2004, **43**, 3277.
59 M. L. Neidig, M. Kavana, G. R. Moran and E. I. Solomon, *J. Am. Chem. Soc.*, 2004, **126**, 4486.
60 J. N. Harvey, M. Aschi, H. Schwarz and W. Koch, *Theor. Chem. Acc.*, 1998, **99**, 95.
61 A. Fiedler, D. Schröder, S. Shaik and H. Schwarz, *J. Am. Chem. Soc.*, 1994, **116**, 10734.
62 P. Nordlund, in *Handbook of Metalloproteins*, ed. I. Bertini, A. Sigel and H. Sigel, Marcel Dekker, Inc, New York, 2001, pp. 461–570.
63 T. A. Dix, G. E. Bollag, P. L. Domanico and S. J. Benkovic, *Biochemistry*, 1985, **24**, 2955.
64 H.-U. Siegmund and S. Kaufman, *J. Biol. Chem.*, 1991, **266**, 2903.
65 A. Bassan, M. R. A. Blomberg and P. E. M. Siegbahn, *Chem. Eur. J.*, 2003, **9**, 106.
66 H. Erlandsen, E. Bjørgo, T. Flatmark and R. C. Stevens, *Biochemistry*, 2000, **39**, 2208.
67 A. Bassan, M. R. A. Blomberg and P. E. M. Siegbahn, *Chem. Eur. J.*, 2003, **9**, 4055.
68 O. A. Andersen, A. Stokka, T. Flatmark and E. Hough, *J. Mol. Biol.*, 2003, **333**, 747.
69 O. A. Andersen, T. Flatmark and E. Hough, *J. Mol. Biol.*, 2002, **320**, 1095.
70 A. Bassan, Ph.D. thesis, Stockholm University, Stockholm, 2004.
71 F. H. Vaillancourt, S. Han, P. D. Fortin, J. T. Bolin and L. D. Eltis, *J. Biol. Chem.*, 1998, **273**, 34887.
72 L. Shu, Y.-M. Chiou, A. M. Orville, M. A. Miller, J. D. Lipscomb and L. Que, Jr., *Biochemistry*, 1995, **34**, 6649.
73 D. M. Arciero and J. D. Lipscomb, *J. Biol. Chem.*, 1986, **261**, 2170.
74 T. D. H. Bugg, *Tetrahedron*, 2003, **59**, 7075.
75 E. L. Spence, G. J. Langley and T. D. H. Bugg, *J. Am. Chem. Soc.*, 1996, **118**, 8336.
76 T. D. H. Bugg and G. Lin, *Chem. Commun.*, 2001, 941.
77 R. J. Deeth and T. D. H. Bugg, *J. Biol. Inorg. Chem.*, 2003, **8**, 409.
78 P. Siegbahn and F. Haeffner, *J. Am. Chem. Soc.*, 2004, **126**, 8919.
79 Y. Uragami, T. Senda, K. Sugimoto, N. Sato, V. Nagarajan, E. Masai, M. Fukuda and Y. Mitsui, *J. Inorg. Biochem.*, 2001, **83**, 269.
80 P. Siegbahn, M. Blomberg and F. Haeffner, unpublished work.
81 S. L. Groce and J. D. Lipscomb, *J. Am. Chem. Soc.*, 2003, **125**, 11780.
82 L. Que, Jr, R. C. Kolanczyk and L. S. White, *J. Am. Chem. Soc.*, 1987, **109**, 5373.
83 S. Ramaswamy, *Handbook of Metalloproteins*, ed. A. Messerschmidt, R. Huber, T. Poulos and K. Wieghardt, John Wiley & Sons, Chichister, 2001, pp. 613–621.
84 A. Bassan, M. R. A. Blomberg, T. Borowski and P. E. M. Siegbahn, *J. Phys. Chem. B*, 2004, **108**, 13031.
85 A. Bassan, M. R. A. Blomberg and P. E. M. Siegbahn, *J. Biol. Inorg. Chem.*, 2004, **9**, 439.
86 K. Chen and L. Que, Jr., *J. Am. Chem. Soc.*, 2001, **123**, 6327.
87 K. Chen, M. Costas, J. Kim, A. K. Tipton and L. Que, Jr., *J. Am. Chem. Soc.*, 2002, **124**, 3026.
88 K. Chen, M. Costas and L. Que, Jr., *J. Chem. Soc., Dalton Trans.*, 2002, 672.
89 A. Bassan, M. R. A. Blomberg, P. E. M. Siegbahn and L. Que, Jr., *J. Am. Chem. Soc.*, 2002, **124**, 11056.